CHAPTER IV
RESULTS AND DISCUSSION

4.1 Relative Comparison between Asphaltic Sludge's Asphaltene (SASPH) and Original Asphaltene (OASPH)

4.1.1 Asphaltic Sludge's Asphaltene Preparation

Asphaltic sludge was prepared using the method described in previous chapter. The precipitated asphaltic sludge is shiny, soft, sticky and rigid film. The viscosity of Venezuela crude oil measured by a rheometer was increased from 0.049 to approximately 166 Pas after asphaltic sludge formed. Asphaltenes precipitated from this asphaltic sludge appear as soft, fine, dark brown powder. It is different from the asphaltene prepares from crude oil, which appeared to be hard and dense black particles. Figure 4.1 shows that the amount of asphaltic sludge's asphaltene (SASPH) precipitated is greater by a factor of approximately 2 than that precipitated from crude oil (OASPH). This may be, in part, due to the fact that an increase in resin and/or lower paraffinic hydrocarbon precipitation as crude oil is in contact with acidic solution and/or the addition of ferric ion during asphaltic sludge precipitation. Metal content analyses were performed in order to validate this hypothesis using ICP measurement.

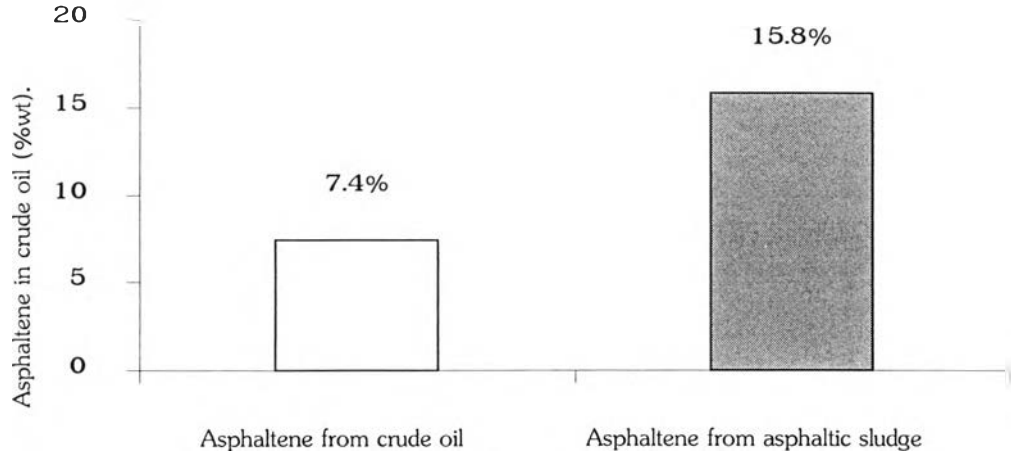

Figure 4.1 The amount of asphaltene obtained from crude oil and from asphaltic sludge.

4.1.2 Metal Analysis of Asphaltic Sludge's Asphaltene and Original Asphaltene

SASPH and OASPH were analyzed for the presence of metal ions. XRAL Activation Services Inc., Ann Arbor, Michigan Arbor, carried out the metal ion analyses. Metal ion content list is presented in Table 4.1. From the third and forth column, the results imply that the amount of ferric ion in SASPH does not affect the steep rise of the amount of asphaltene. Komaethwarakul (1998) found that lower polar asphaltene subfractions have lower iron, nickel, and vanadium contents and *vice versa*. These metal ions were considerably attained in asphaltenes. The experimental results show that SASPH has lower iron, nickel, and vanadium than OASPH. This indicates that SASPH contains lower polar subfraction than OASPH. These results confirm the hypothesis regarding co-precipitation of resin and lower paraffinic hydrocarbons.

Table 4.1 Metal ions content in asphaltene using ICP technique

Element	Units	Asphaltene from		Asphaltene Subfraction	
		asphaltic sludge	crude oil	F70/30	F60/40
Al	%	<0.01	<0.01	<0.01	<0.01
Ba	PPM	30	20	10	20
Be	PPM	<5	<5	<5	<5
Ca	%	<0.01	<0.01	<0.01	<0.01
Cd	PPM	<10	<10	<10	<10
Co	PPM	<10	<10	<10	<10
Cr	PPM	40	<10	<10	<10
Cu	PPM	10	10	10	<10
Fe	**%**	**1.91**	**0.02**	**0.03**	**0.01**
K	%	0.03	<0.01	<0.01	<0.01
Mg	%	<0.01	<0.01	<0.01	<0.01
Mn	PPM	60	<10	<10	<10
Ni	**PPM**	**190**	**260**	**330**	**260**
P	%	<0.01	<0.01	<0.01	<0.01
Pb	PPM	<20	<20	<20	<20
Sb	PPM	<50	<50	<50	<50
Sc	PPM	<5	<5	<5	<5
Sn	PPM	<50	<50	<50	<50
Sr	PPM	<10	<10	<10	<10
Ti	%	<0.01	<0.01	<0.01	<0.01
V	**PPM**	**820**	**1300**	**1600**	**1300**
W	PPM	<50	<50	<50	<50
Y	PPM	<5	<5	<5	<5
Zn	PPM	50	240	200	680
La	PPM	<10	<10	<10	<10

4.1.3 Morphology Study

Morphology of the precipitates of asphaltenes were studied using scanning electron microscope (SEM). The SEM images of OASPH and SASPH show clear distinctions in the microstructure of the two fractions as illustrated in Figure 4.2.

Figure 4.2a shows the un-ordered, fibrous, and more porous structure of the SASPH and Figure 4.2b shows a planar surface on the OASPH. Pumpaisanchai (1995) found that a low polar asphaltene subfraction is fibrous and more porous than a high polar subfraction. However, the results of Pumpai sanchai contradict with the results obtained in this study by which. SASPH shows high polarity together with fibrous structure.

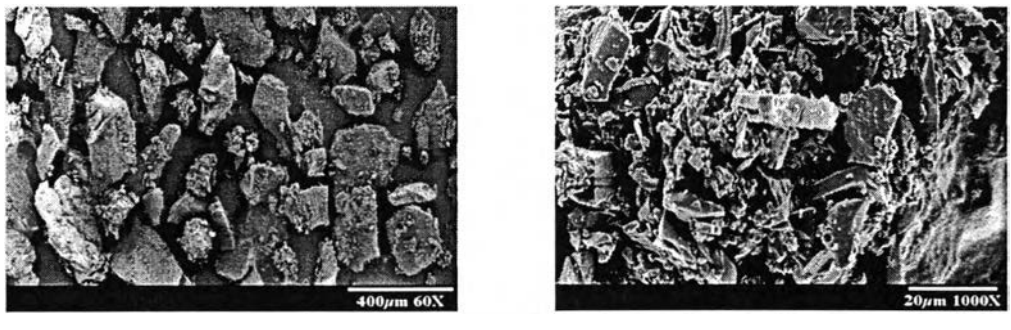

a) SEM images of OASPH.

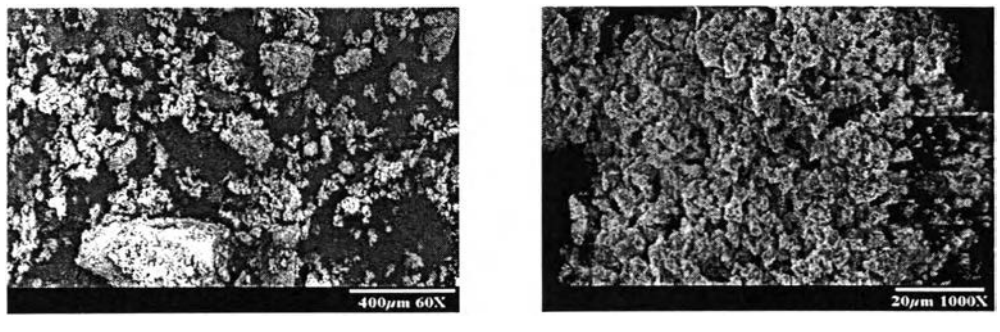

b) SEM images of SASPH.

Figure 4.2 SEM images of asphaltene precipitated.

4.1.4 Asphaltene Dissolution

Studies of asphaltene dissolution kinetics were carried out on unfractionated asphaltene precipitated using the apparatus described. Ten milligrams of asphaltene precipitated was used in each experiment. The solvent used was 5% by wt.DBSA in heptane solvent at a flow rate of 1.5 ml/min. The temperature used in each experiment was 17°C.

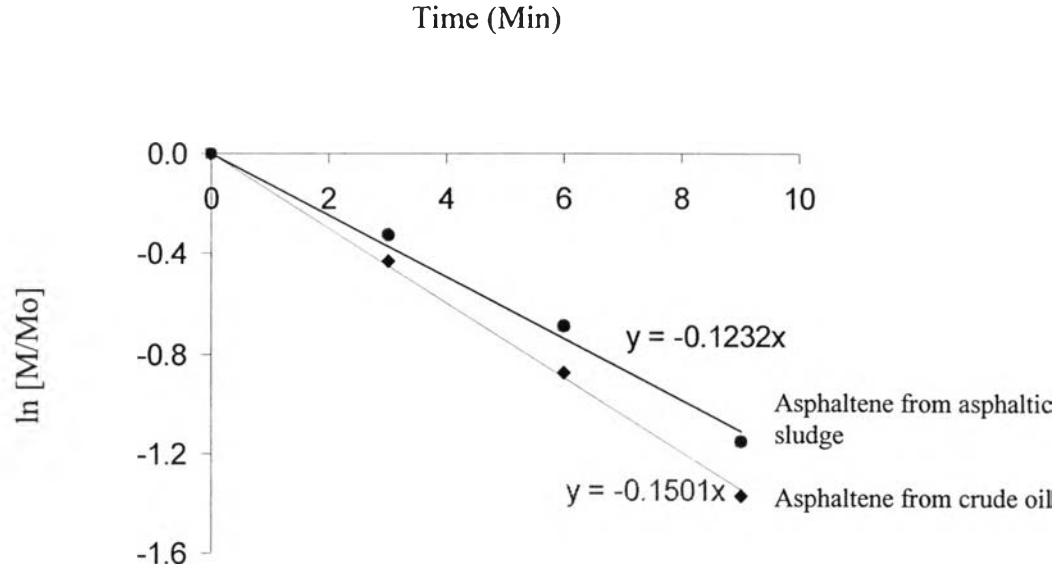

Figure 4.3 Determination of asphaltene dissolution rate constants.

Figure 4.3 shows data analysis for the rate of asphaltene dissolution using the first-order dissolution. The first-order model provides a satisfactory fit to the experimental data. The pseudo first order dissolution rate contents were found to be 0.1232 and 0.1501 min^{-1} for SASPH and OASPH respectively. This indicates that the asphaltene in asphaltic sludge can cause more severe problems.

4.1.5 Asphaltene Fractionation

SASPH was fractionated using the method described in preceding chapter. For relative comparison, OASPH extracted from the same batch of crude oil was used as a standard. The results of these asphaltenes are presented in Figure 4.4. The SASPH was found to be about 70% in F60/40 to F40/60, while being less than 5% for OASPH. It can be interpreted that the asphaltene from asphaltic sludge precipitated by FeCl3/HCl greatly increases the relative amount of the higher polarity fraction. This may be due to SASPH containing higher functional groups, and/or higher in aromaticity than OASPH.

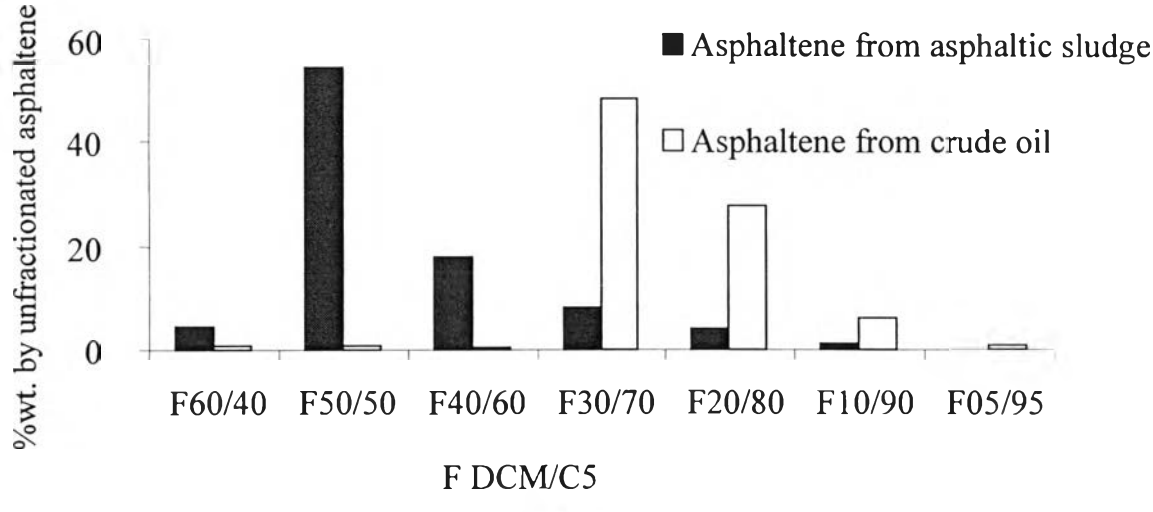

Figure 4.4 Asphaltene subfraction of OASPH and SASPH.

4.1.6 Functional Group Analysis

Unfractionated asphaltene powders from both asphaltic sludge and crude oil were characterized using FTIR spectroscopy. The FTIR spectra of the precipitated asphaltene are shown in Figure 4.5. They are similar, but it is found that SASPH is absorbed stronger at 1600 cm^{-1} and in the range of 3100-3600 cm^{-1} , which represent double bond stretching or aromatic ring and hydrogen-bonding band respectively. This strong absorption is due to more unsaturated hydrocarbon and hetero-atom in SASPH accounting for high polarity of asphaltene molecules. These FTIR spectra also confirm that SASPH

contains high polarity fractions. Peak positions and assignments of asphaltene molecules are listed in Table 4.2.

Table 4.2 IR Band Assignments

Wave Number (cm^{-1})	Assignment
1450	-C-CH_3-, -CH_2- Stretching
1600	Aromatic or –C=C- Stretching
2850, 2920	CH_2 Stretching
2950	CH_3 Stretching
3480	Free N-H Stretching
3100-3600	H-Bonding Stretching

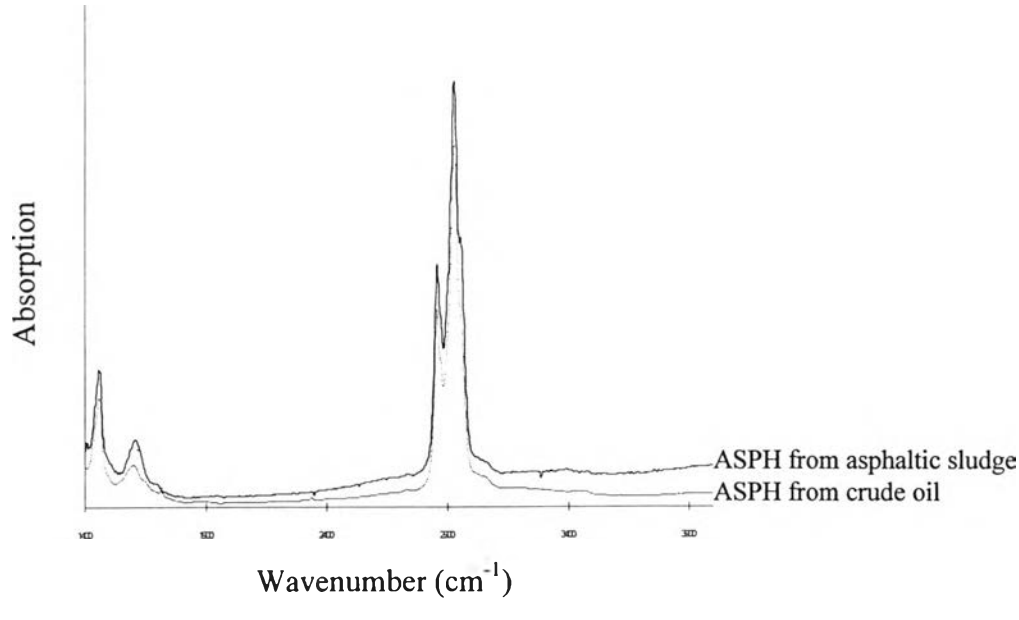

Figure 4.5 FTIR spectra of OASPH and SASPH.

4.1.7 Asphaltene Structure Analysis

^{1}H-NMR spectrum of asphaltene precipitated from both asphaltic sludge and crude oil as illustrated in Figures 4.6 and 4.7 exhibited five centered at 0.95, 1.35, 1.8, 2.55, 7.4 ppm which corresponded to the fractional distribution of protons among paraffinic methyl, paraffinic methylene, naphthenic, benzylic, and aromatic attachments. The experiments show that asphaltene from asphaltic had photon among naphthenic attachment greater than that from crude oil. This may be due to co-precipitation of lower hydrocarbon molecules and/or modification of asphaltene molecules itself.

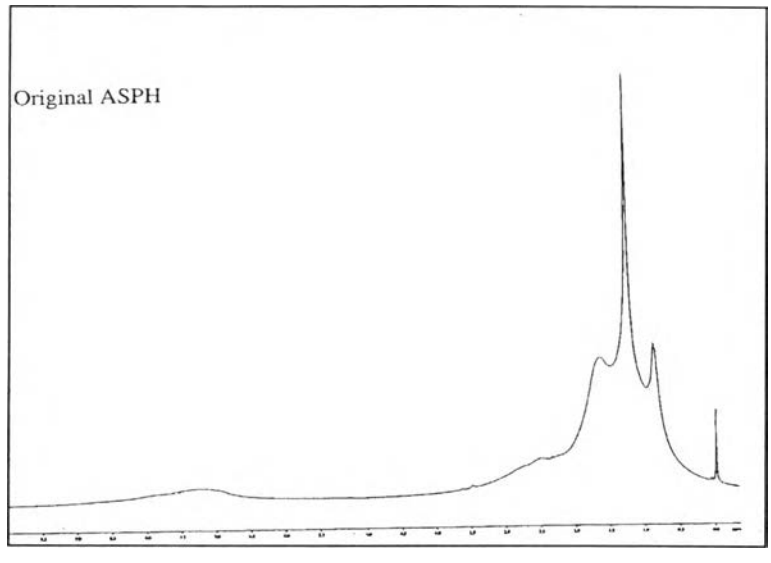

Figure 4.6 ^{1}H-NMR spectrum of OASPH.

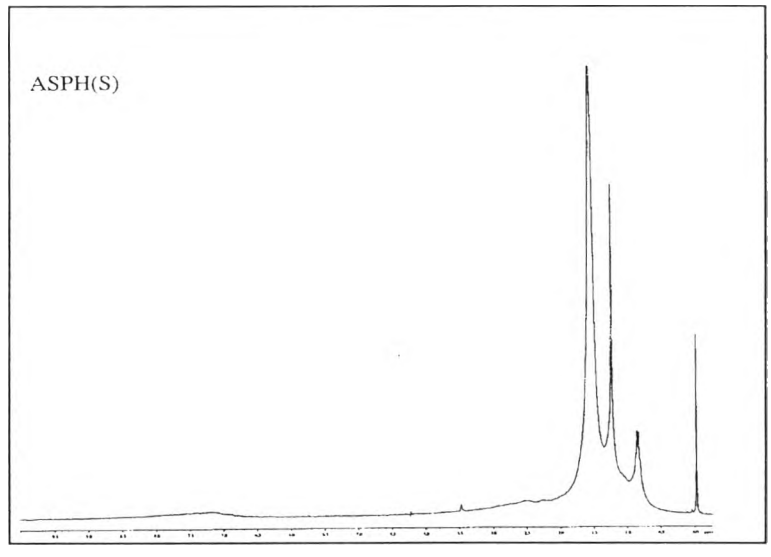

Figure 4.7 ^{1}H-NMR spectrum of SASPH.

4.2 Asphaltene from Different Asphaltic Sludge Precipitating Conditions

Asphaltenes were extracted from asphaltic sludges precipitated from crude oil using acidic solution varying hydrochloric acid and ferric chloride concentration. The effect of aging of asphaltic sludge was also investigated.

4.2.1 Asphaltene Dissolution

Dissolution of this asphaltene were carried out in a differential reactor using the apparatus described in chapter 3. Ten milligrams of asphaltene precipitated were used in each experiment. The solvent used was 5% by wt.DBSA in heptane solvent at a flow rate of 1.5 ml/min. The temperature in each experiment was 17°C.

A list of dissolution rate constants of SASPH with different precipitating conditions presented in Table 4.3. It was found that asphaltene did not form asphaltic sludge after crude oil contacted with ferric chloride solution and dissolution rate constant was 0.1542 min^{-1}. This can be indicated that

ferric chloride solution did not affect original asphaltene in crude oil. This result also confirmed the asphaltene fractionation result. The dissolution rate constant of asphaltene obtained from asphaltic sludge depends mainly on ferric ion concentration in hydrochloric solution and aging of the asphaltic sludge.

Table 4.3 Asphaltene Dissolution Rate Constant List

Solution Added		Aging	Dissolution Rate
[FeCl3] (PPM)	[HCl] (M)	(Days)	Constant (min-1)
nil	nil	0.4	0.1501
9000	nil	10	0.1542
nil	4.4	10	0.1075
nil	4.4	15	0.0599
9000	4.4	0.4	0.1232
9000	4.4	10	0.0297
9000	4.4	15	0.0245

4.2.2 Asphaltene Fractionation

The precipitated asphaltene was fractionated using the method described in Chapter 3. Figures 4.8-4.11 show asphaltene subfractions of each asphaltenes. The dissolution rate constant of asphaltene decreased with increasing of high polar asphaltene subfractions. These results were confirmed by Pumpaisanchai's report (1995). She reported that high polar subfraction had low asphaltene dissolution rate constant. An increase in high polar subfraction might be due to asphaltene modification via acidic solution leading to have more polar functional group. When asphaltenes have higher functional groups implying to stronger asphaltene-asphaltene interactions, it causes hydrogen bonding and π-π electron interaction (Mansoori, 1996). This confirmed more difficulty of asphaltene dissolution results. Aging of asphaltic sludge decreases asphaltene dissolution rate constant and also increases high polar asphaltene

subfractions. For relative comparison, asphaltene extracted from different asphaltic sludge ages were prepared. The results of these asphaltenes are presented in Figure 4.10. The asphaltic's asphaltenes were precipitated by the presence of ferric ion in acidic solutions. It was found that asphaltenes increased in high polar subfracions and decreased in low polar subfraction against the increasing of asphaltic ages. The mentioned situation of asphaltenes can be due to the changing of the structure or chemical reaction themselves. The reactions that might take place can be proposed as follows:

i) The polymerization of asphaltene: this leads to the increasing of aromatic sheet size of asphaltene molecules. These represent higher asphaltene-asphaltene $\pi-\pi$ electron interactions and polarity. This reaction can explain the difficulty of asphaltene dissolution and the increasing of hydrogen bonding between asphaltene after aging of asphaltic sludge which represent in FTIR spectrum of asphaltenes (Figure 4.12).

$$m\,(\text{Asphaltene}) \xrightarrow{\text{Acidizing}} \{\text{Asphaltene}\}_m$$

ii) The co-polymerization of asphaltene and resin: it will form the bigger asphaltene molecular sizes, which are similar to the first reason. This reaction can be explained the increase in the amount of asphaltene obtained from crude oil.

$$m\,(\text{Asphaltene}) + n\,(\text{Resin}) \xrightarrow{\text{Acidizing}} \{\text{Asphaltene-Resin}\}_{m,n}$$

iii) The polymerization of resin alone: this may also take place in presence of higher asphaltene yield. Resins may polymerize each other, after that will form bigger molecules and behave like the property of asphaltene.

$$n\,(\text{Resin}) \xrightarrow{\text{Acidizing}} \sim(\text{Resin})_n\sim \quad (\text{Asphaltene Like})$$

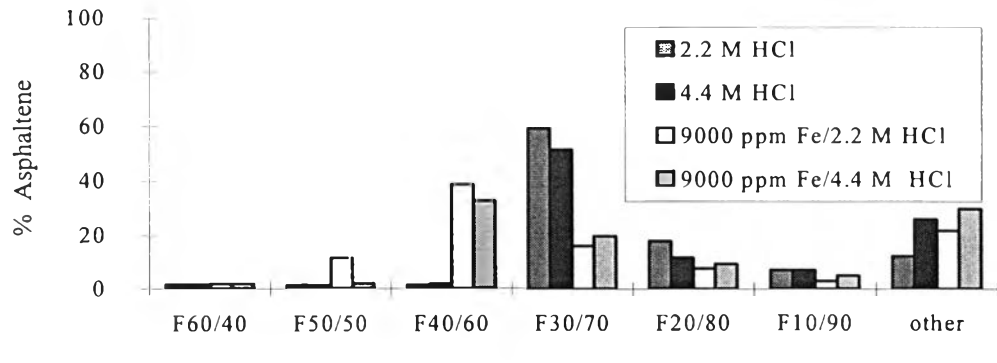

Figure 4.8 Effect of HCl concentration on asphaltene subfraction.

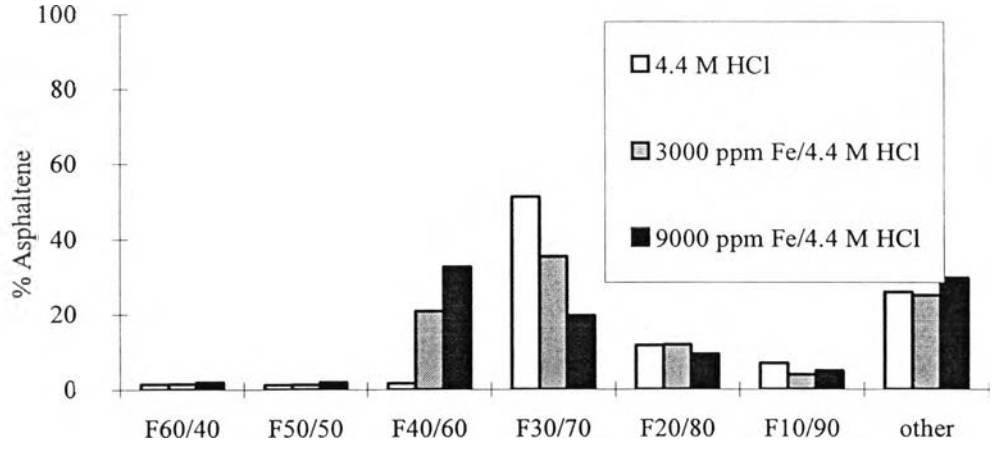

Figure 4.9 Effect of ferric ion concentration on asphaltene subfraction.

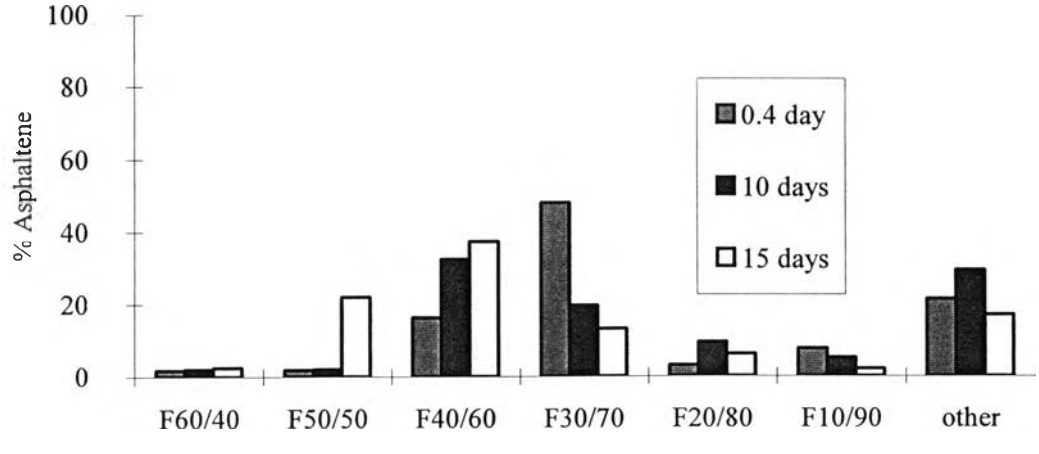

Figure 4.10 Aging of asphaltic sludge on asphaltene subfraction.

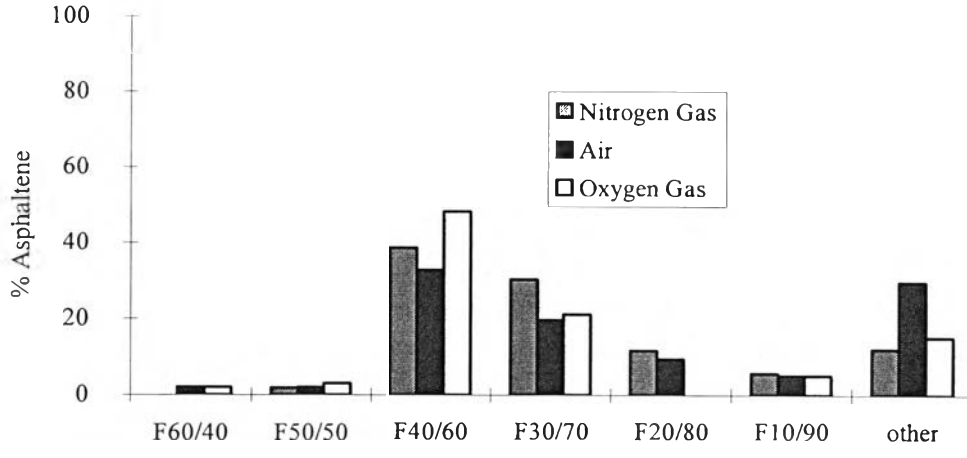

Figure 4.11 Effect atmosphere on asphaltene subfraction.

4.2.3 Functional Group Analysis

Precipitated asphaltenes obtained from different asphaltic sludge ages were characterized using FTIR spectroscopy. The FTIR spectra of the precipitated asphaltene are shown in Figure 4.12 They are similar, but it was found that aging of asphaltic sludge tended to have higher absorption at 1600 cm^{-1} and in the range of 3100-3600 cm^{-1} representing aromatic ring stretch and hydrogen-bonding band respectively. This strong absorption is due to more heteroatom, functional group in asphaltene and/or unsaturated hydrocarbon in asphaltene accounting to higher polarity of asphaltene molecule. These FTIR spectra confirmed the result from fractionation study, about increasing of polarity of asphaltene from aging of asphaltic sludge and difficulty of asphaltene obtained after aging of asphaltic sludge. Peak positions and assignment of asphaltene molecule are listed in Table 4.2.

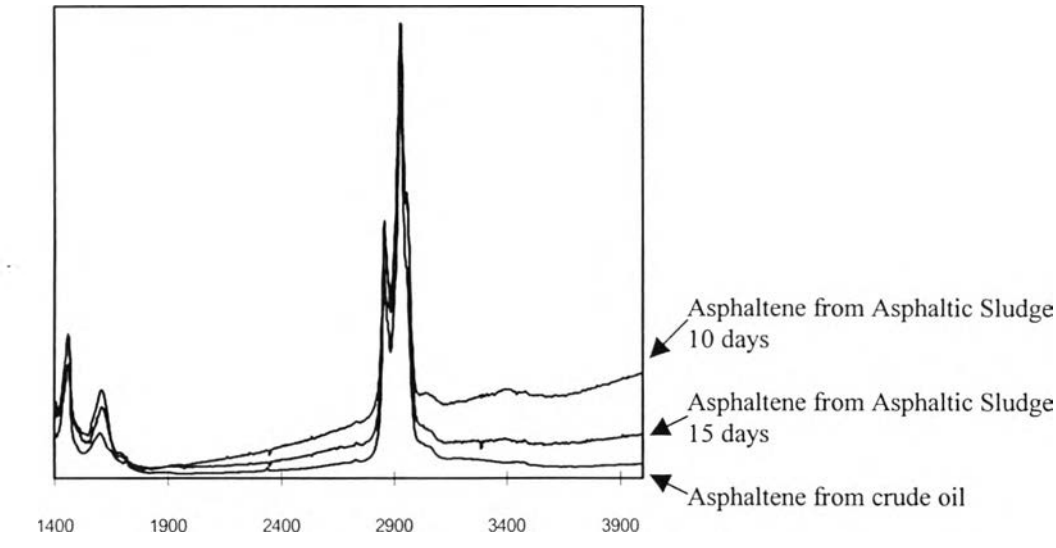

Figure 4.12 FTIR spectra of asphaltene from aging of asphaltic sludge study.

4.2.4 Structure analysis of asphaltene from asphaltic sludge precipitated by acidic solution in the presence and absence of ferric ion

^{1}H-NMR spectrum of SASPH in the presence and absence of ferric in acidic solution are presented in Figure 4.13 and 4.14. These asphaltenes exhibit five centered at 0.95, 1.35, 1.8, 2.55, and 7.4 ppm corresponding to the fractional distribution of protons among paraffinic methyl, paraffinic methylene, naphthenic, benzylic, and aromatic attachments as described in previous section. The results show that asphaltene from asphaltic sludge precipitated by acidic solution in presence of ferric ion had photon among naphthenic, greater than that precipitated by hydrochloric acid alone. This may be due to co-precipitation of resin and lower hydrocarbon molecules and/or modification of asphaltene molecule and/or ferric ion in solution forming a complex with asphaltene and/or resin. This may be one possible reason that can explain the increase in asphaltene yield.

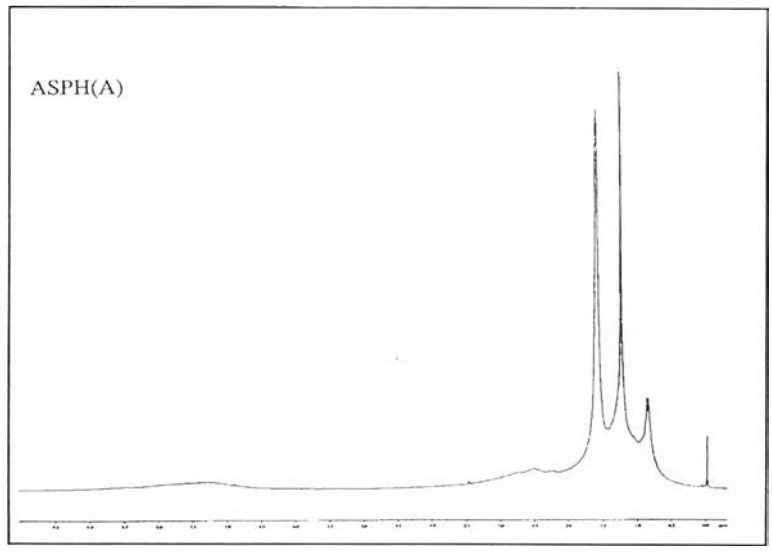

Figure 4.13 ^{1}H-NMR spectrum of SASPH precipitated by 4.4 M hydrochloric acid.

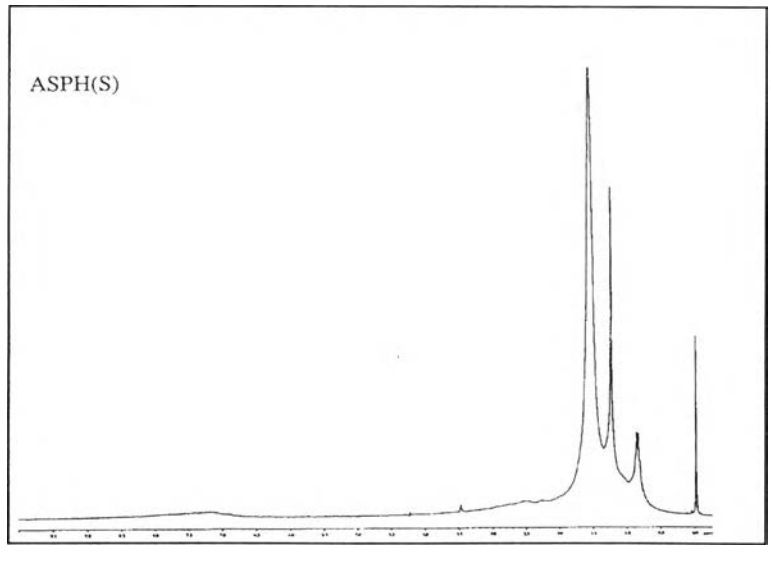

Figure 4.14 ^{1}H-NMR spectrum of SASPH precipitated by acidic solution in the presence of ferric ion.

4.3 Asphaltene Re-precipitation

In order to study the effect of acid system to asphaltene, the experiments were performed by re-dissolving asphaltene obtained directly from crude oil with pure toluene and then re-precipitating it with acid solution. Prepared asphaltenes were separated and fractionated.

4.3.1 Asphaltene Fractionation and Dissolution

It was found that an increase of asphaltene polarity occurred after asphaltene contacted with acidic solution as shown in Figure 4.15. These re-precipitated asphaltenes had lower dissolution rate constant than original asphaltene. Asphaltene dissolution rate constants were decreased from 0.1501 (for original asphaltene) to 0.0641 and 0.0401 min^{-1} (for re-precipitated asphaltene) in the presence and absence of ferric ion in acidic solution respectively. It can be proposed that asphaltene polymerization might take place due to increasing of asphaltene polarity and/or taking place of other asphaltene reaction such as dehydrogenation of asphaltene molecule by acid. Adding of ferric chloride to acidic solutions did not affect the dissolution rate. This may be because asphaltene molecule cannot combine with ferric ion to form ferric-asphaltene complex.

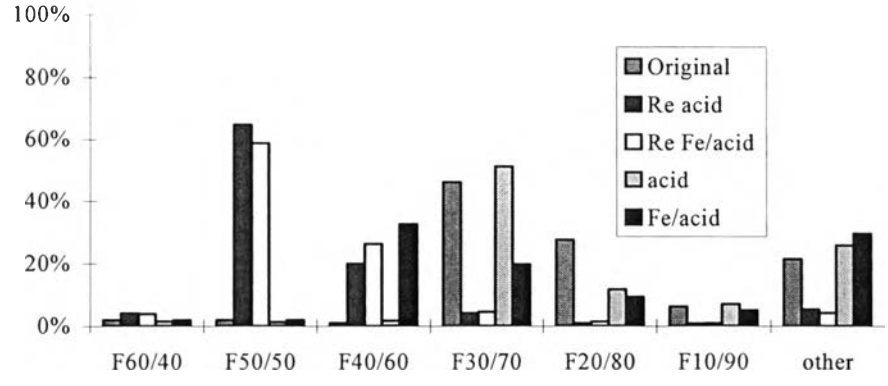

Figure 4.15 Re-precipitated asphaltene, using acidic solutions.

4.3.2 Asphaltene Structure Analysis

^{1}H-NMR spectrum of re-precipitated by in presence of ferric ion and absence of ferric ion in acidic solution are presented in figure 4.16 and 4.17. These asphaltenes exhibit the same five centered at 0.95, 1.35, 1.8, 2.55, and 7.4 ppm as SASPH. These correspond to the fractional distribution of protons among paraffinic methyl, paraffinic methylene, naphthenic, benzylic, and aromatic attachments as described in previous section. The results show that re-precipitated asphaltene by acidic solution in presence and absence of ferric ion in acidic solution had greater photon among naphthenic and lower photon among paraffinic than that from original asphaltene. This may be due to the changing of asphaltene molecule and/or ferric ion in solution formed a complex with asphaltene and/or resin or low paraffinic hydrocarbon. This may be a possible reason that can explain the increase of asphaltene polarity.

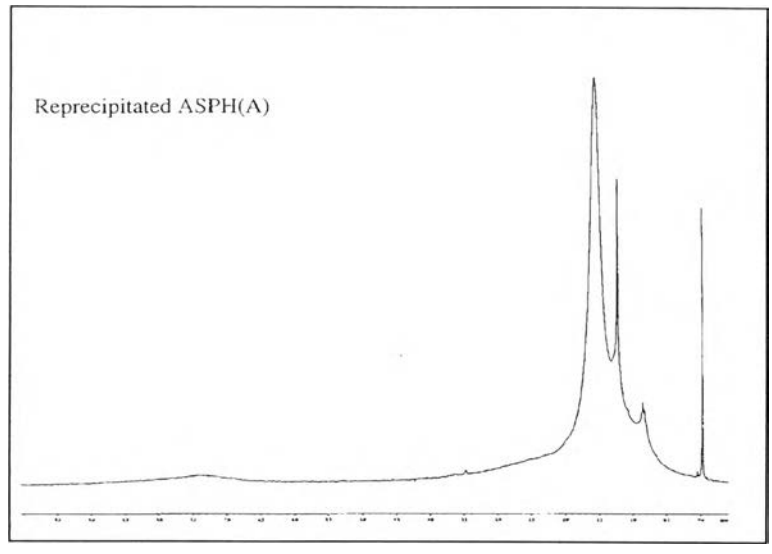

Figure 4.16 H-NMR spectrum of re-precipitated by 4.4 M hydrochloric acid solution alone.

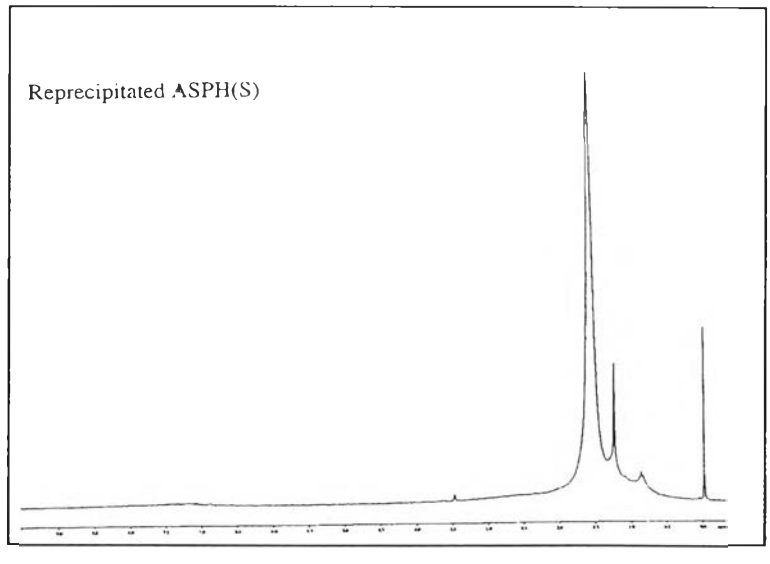

Figure 4.17 H-NMR spectrum of re-precipitated asphaltene by acidic solution in presence of ferric ion.

4.3.3 Aromaticity Analysis

Original and re-precipitated asphaltene were analyzed the contants of carbon, hydrogen, sulfur, and nitrogen using elemental analyzer (chemical analyzer). Table 4.4 presents the percent element and the atomic ratios for precipitated asphaltene.

Table 4.4 Percent Element and Atomic Ratio for Asphaltene

Asphaltene	Element					Atomic Ratio			
	C	H	N	S	O	H/C	N/C	S/C	O/C
OASPH	77.59	8.97	0.19	5.12	8.13	1.39	0.002	0.025	0.079
Re-precipitated OASPH using									
-$FeCl_3$/HCl	80.56	8.15	0.83	3.49	6.97	1.21	0.008	0.016	0.065
-HCl	80.84	8.22	1.23	3.47	6.24	1.22	0.011	0.016	0.058

The experimental results show that asphaltene re-precipitation decreased hydrogen/carbon atomic ratio and number closed to one. It can be interpreted that acid treatment might increase asphaltene aromaticity. This may be due to the changing of the structure of asphaltene.